RSC Advances

ROYAL SOCIETY OF CHEMISTRY

www.rsc.org/advances

Phenolic Metabolites from Mangrove-Associated *Penicillium pinophilum* Fungus with Lipid-Lowering Effects

Chongming Wu,[a] Yang Zhao,[b] Ran Chen,[a] Dong Liu,[b] Mingyue Liu,[a] Peter Proksch,[c] Peng Guo,[a,*] Wenhan Lin[b,*]

[a]Pharmacology and Toxicology Research Center, Institute of Medicinal Plant Development, Chinese Academy of Medical Sciences, Peking Union Medical College, Beijing 100193, P. R. China

[b]State Key Laboratory of Natural and Biomimetic Drugs, Peking University, Beijing 100191, P.R. China

[c]Institute für Pharmazeutische Biologie und Biotechnologie, Heinrich-Heine-Universität Düsseldorf, Universitätsstr. 1, Geb.26.23, 40225 Düsseldorf, Germany

*Corresponding authors:

W. Lin, Tel: +86-10-82806188, Fax: +86-10-82802724. E-mail: whlin@bjmu.edu.cn

P. Guo, Tel./Fax: +86-10-57833235. E-mail: pguo@implad.ac.cn

Chemical examination of the mangrove-associated fungus *Penicillium pinophilum* (H608) resulted in the isolation of 16 phenolic metabolites, including a new metabolite namely 5'-hydroxypenicillide (**1**). The structure of new compound was determined by extensive spectroscopic analyses, in association with the Mosher method for the configurational assignment. All compounds were tested for the inhibitory effects against oleic acid (OA)-elicited lipid accumulation in HepG2 cells, while eight compounds (**4**, **7-8**, **11-15**) exhibited the inhibition toward lipid accumulation at a dose of 10 μM with no cytotoxic effect. Further investigation revealed six compounds (**4**, **11-15**) significantly suppressed intracellular total cholesterol (TC) and triglycerides (TG). A real-time quantitative PCR indicated that compounds **4**, **11**, **13-15** dramatically decreased the expression of fatty acid synthase (FAS), acetyl-CoA carboxylase (ACC) and 3-hydroxy-3-methylglutaryl-CoA reductase (HMGR) in association with up-regulation of carnitinepalmitoyl transterase-1 (CPT-1). In addition, seven compounds (**4**, **8**, **11**, **13-16**) significantly reduced oxidized low-density lipoprotein stimulated lipid accumulation in RAW264.7 cells. Mechanistic study revealed that compounds **14-16** remarkably decreased CD36 and SR-1 transcription, while compounds **4** and **15** dramatically up-regulated PPARγ, LXRα and ABCG1 to promote cholesterol efflux. This work provided a group of new chemical entity as the promising leads for the development of hypolipidemic and anti-atherosclerotic agents.

Keywords: Fungus; *Penicillium pinophilum*; Phenolic compounds; Structural elucidation; Lipid-lowering effect; Regulation of lipogenic genes

1. Introduction

Hyperlipidemia is known as abnormally elevated levels of lipids (high cholesterol and/or triglyceride levels) and/or lipoproteins in the blood, which raised the risk of cardiovascular (atherosclerosis and coronary heart diseases) and heart diseases.[1-5] In addition, hyperlipidemia also aggravated other pathological conditions such as hypothyroidism and chronic kidney dysfunction.[6] In the other side, atherosclerosis,[7] a progressive disease that characterized by the formation and accumulation of lipid plaques in the arteries and by inflammatory responses, resulted in insufficient blood supply to organs and tissues, that induced the deaths of cardiovascular disease.[8,9] Low-density lipoprotein (LDL) plays a key role for the accumulation of extracellular and intracellular lipids in the arterial intima to develop atherogenesis.[10,11] Foam cell formation is a main determinant of atherosclerotic lesions, in which macrophages express scavenger receptors on their plasma membranes and uptake oxidized LDL.[12] Foam cells also secrete various inflammatory cytokines to accelerate the development of atherosclerosis. For instance, scavenger receptors CD36, SR-A1 and SR-A2 bind to and uptake excess oxLDL into macrophages,[13] leading to the accumulation of excess cholesterol, which is toxic to cells. ATP-binding cassette (ABC) transporters (ABCA1 and ABCG1) induced the reverse cholesterol transport (RCT) pathway by mediating the translocation of cholesterol across cellular bilayermembranes.[14-16] ABCA1 promotes the efflux of cholesterol to lipid-poor apolipoproteins such as apolipoprotein A1 (apoA1), while ABCG1 mediated cholesterol efflux to high-density lipoprotein (HDL).[17-19] The expression of ABCA1 and ABCG1 is regulated by proliferator-activated receptor gamma (PPARγ)-dependent and liver X receptor alpha (LXRα)-dependent pathways, respectively.[20,21] The marketed lipid-lowering agents with beneficial therapeutic effects are mainly classified into statins and fibrates,[22]

while rosiglitazone is used for the treatment of atherogenesis through the stimulation of cholesterol efflux by up-regulating ABCA1 to prevent foam cell formation. Among the "statin" derivatives, compactin (mevastatin) is the first fungal metabolite with a PKS-based scaffold to be isolated from fungi *Penicillium citrinum* and *P. brevicompactum*., and it performed as a specific inhibitor of HMG-CoA reductase with highly effective in lowering plasma cholesterol levels in animals and men.[23] The fungal product lovastatin (mevinoline) structurally related to compacin as isolated from the fungus *A. terreus*, was the first marketed "statin" drugs.[24] Microbial transformation of compactin resulted in the lactone ring opened to form pravastatin, which showed a reduction in side effects compared with lovastatin and simvastatin.[25] Thus, natural products are an excellent strategy for developing future effective and safe hypolipidemic and anti-atherosclerotic drugs. With the aim of discovering new bioactive natural products with lipid-lowering effects from marine-derived microorganisms, a cell model-based bioassay was performed. The results demonstrated that a mangrove soil derived fungus *Penicillium pinophilum* can reduce lipid accumulation. Chromatographic separation of an active lipid-lowering ethyl acetate (EtOAc) fraction from the fungus led to the isolation of 16 phenolic compounds (Fig. 1). In this paper, we report the inhibitory effects of the phenolic analogues on lipid-lowering effects and of oxLDL-induced foam cell formation, in addition to the potential mechanisms in RAW264.7 macrophages.

2. Experimental

2.1. General procedures

Optical rotations were measured by an Autopol III automatic polarimeter (Rudolph Research Co., Ltd.). IR spectra were measured on a Thermo Nicolet Nexus 470 FT-IR spectrometer. The ^{1}H and ^{13}C NMR spectra were recorded on a Bruker

Avance-400FT NMR spectrometer using TMS as an internal standard. HRESIMS spectra were obtained on a Bruker APEX IV 70 eV FT-MS spectrometer and on a Thermo DFS spectrometer using a matrix of 3-nitrobenzyl alcohol. EIMS (70 eV) were recorded on a Finnigan MAT 95 mass spectrometer. Column chromatography was carried by silica gel (160-200, 200–300 mesh), and HF_{254} silica gel for TLC was obtained from Qingdao Marine Chemistry Co. Ltd. Sephadex LH-20 (18–110 μm) was obtained from Pharmacia. HPLC was performed on Alltech 426 pump employing an UV detector, and the prevail C_{18} column (5 μm) was used for semipreparative HPLC separation. Chiral-phase column (Phenomenex Lux, cellulose-2, 250 × 10 mm, 5 μm) was used for chiral analysis. 25-[*N*-[(7-nitrobenz-2-oxa-1,3-diazol-4-yl)-methyl] amino]-27-norcholesterol (25-NBD cholesterol), MTT, digitonin, simvastatin, rosiglitazone, Oil Red O and Dulbecco's modified Eagle's medium (DMEM) were purchased from Sigma-Aldrich, Inc. (St. Louis, MO, USA). An intracellular cholesterol assay kit was purchased from Jian Cheng Biotechnology Company (Nanjing, China). Human oxLDL, ApoA1 and HDL were obtained from Yiyuan Biotechnologies (Guangzhou, China). A total RNA extraction reagent (RNAiso Plus), a Prime Script RT reagent kit, and a SYBR-Green PCR kit were purchased from Transgene Biotech, Inc. (Beijing, China). A luciferase assay kit was purchased from Promega Inc. (Beijing, China).

2.2. Fungal strain and identification

Fungus *Penicillium pinophilum* (H608) was isolated from the mangrove sediment, which was collected from Xiamen coastline, in May 2012. The strain was identified by comparing the morphological character and 18S rDNA (ITS) sequence with those of standard records. The morphological examination was performed by scrutinizing the fungal culture, the mechanism of spore production, and the characteristics of the

spores. For inducing sporulation, the fungal strains were separately inoculated onto potato dextrose agar. All experiments and observations were repeated at least twice leading to the identification of the strain H608 as *Penicillium pinophilum.* The strain H608 was deposited at the State Key Laboratory of Natural and Biomimetic Drugs, Peking University, China, with the GenBank (NCBI) accession number KP901304.

2.3. Fermentation.

The fermentation was carried out in 30 Fernbach flasks (500 mL), each containing 100 g of rice. Distilled H_2O (100 mL) was added to each flask, and the contents were soaked overnight before autoclaving at 15 psi for 30 min. Spore inoculum was prepared by suspending the seed culture in sterile, distilled H_2O to give a final spore/cell suspension of 1×10^6/mL. After cooling to room temperature, each flask was inoculated with 5.0 mL of the spore inoculum and incubated at 25 ℃ for 40 days.

2.4. Extraction and isolation.

The fermented material was extracted successively with EtOAc (3 × 500 mL). The EtOAc extract was evaporated to dryness under vacuum to afford a crude residue (11.7 g), which was then subjected to silica gel (200–300 mesh) vacuum column chromatography, eluting with PE/EtOAc (from 5:1 to 0:1, gradient) to obtain six fractions (F1 to F6). The ^{1}H NMR spectra informed that fraction F4 contains the components featured by phenolic compounds. Thus, fraction F4 (3.0 g) was chromatographed over C_{18} gel (ODS, MeOH/H_2O = 3:1) to obtain four subfractions (SF4a-SF4d). SF4c (1.43 g) was purified on a silica gel column using hexane/acetone = 5:2 as an elutant to obtain **1** (18.0 mg), **2** (24.5 mg), **3** (7.6 mg), **4** (18.2 mg), **5** (8.7 mg), and **6** (24.8 mg). SF4b (310 mg) was subjected to RP-HPLC with a mobile phase of MeCN/H_2O = 2:1 (2 ml/min) to yield **16** (17.6 mg), **15** (7.8 mg), and **14**(23.5 mg). SF4d (110 mg) was subjected to RP-HPLC

with a mobile phase of MeCN/H_2O = 3:1 (2 ml/min) to yield **7** (27.1 mg), **8** (17.2 mg), **9** (13.5 mg), **10** (11.7 mg), **11** (8.7 mg), **12** (6.7 mg), and **13** (18.3 mg).

5'-Hydroxypenicillide (**1**): white solid. $[\alpha]^{25}_{D}$–27.5 (*c* 0.05, MeOH); UV (MeOH)λ_{max} (log ε) 217 (1.74), 280 (1.12) nm; IR (KBr)ν_{max} 3388, 2958, 1732, 1598, 1468, 1357, 1294, 1206 cm^{-1}; ^1H and ^{13}C NMR data, see Table 1; HRESIMS *m*/*z* 389.1594 $[M + H]^+$ (calcd for $C_{21}H_{25}O_7$, 389.1600).

2.5. MPA esterification and 9-AMA esterification of 1

Compound **1** (4 mg, 0.01 mmol) was dissolved in dimethyl carbonate (4 mL), then DBU (0.6 mmol) was added. The solution was kept at 90 °C under magnetic stirring and monitored by TLC. After disappearance of **1**, the solvent was evaporated under reduced pressure. The residue was solubilized with ethyl acetate (10 mL) and treated with a solution of 1N HCl (5 mL). The final products were extracted with ethyl acetate (3 × 10 mL), the reunited organic extracts were washed with a saturated solution of NaCl and dried over Na_2SO_4. After filtration and evaporation of the solvent, methylated compound was purified by chromatography on column by using silica gel (160-200 mesh) eluting with CH_2Cl_2/CH_3OH (5:2) to yield 11-methylated **1** (3.8 mg).

Both (*R*)- and (*S*)-MPA esters of 11-methylated **1** were obtained by the treatment of 11-methylated **1** (0.9 mg, respectively) with (*R*)- and (*S*)-MPA (3.1 mg), dicyclohexylcarbodiimide (3.9 mg) in dry $CDCl_3$ (0.6 ml) catalyzed with dimethylaminopyridine (2.32 mg) and stirred at rt overnight. The MPA esters, **1a** (1.4 mg) and **1b** (1.6 mg), were purified by semipreparative HPLC using MeCN (100%) as a mobile phase.

Esters **1c** and **1d** were prepared separately by treatment of 11-methylated **1** (1 mg) with the corresponding (*R*)- and (*S*)-9-AMA acids (1.1 equiv) in the presence of EDC

(1.1 equiv) and DMAP in dry CH_2Cl_2, under a N_2 atmosphere. The reaction was stirred at room temperature for 12 h. The organic layer was washed sequentially with H_2O, HCl (1 M), H_2O, $NaHCO_3$ (sat), and H_2O, then dried (Na_2SO_4) and concentrated under reduced pressure to obtain the corresponding ester. Final purification was achieved by column chromatography on silica gel 160-200 mesh eluting with hexane-EtOAc (3:1) to yield **1c** (1.2 mg) and **1d** (1.5 mg).

2.6. HepG2 cell culture

HepG2 cells, which originated from the American Type Culture Collection (ATCC) (Manassas, VA, USA) and obtained from the Peking Union Medical College, were maintained in DMEM medium containing 10% fetal bovine serum (FBS) at 37 ^{o}C and 5% CO_2. Before treatment, cells were kept in serum-free DMEM for 12 h then incubated with the indicated concentration of SN12 or with simvastatin (10 μM) in DMEM containing oleic acid (100 nM) for 24 h. The blank group was incubated with serum-free DMEM alone. Oil red O staining was performed as previous reported and the intracellular contents of total lipid, total cholesterol and triglyceride were determined by kits according to manufacturer's instructions.

2.7. Oleic acid (OA)-elicited lipid accumulation.

HepG2 liver cells were maintained in DMEM medium supplemented with penicillin/streptomycin (100 μg/mL) and 10% fetal bovine serum. The cells with 70-80% confluence were incubated in DMEM/oleic acid (100 μM) for 12 h and then were treated with the compounds (each, 10 μM) and the positive control simvastatin in DMEM/100 μM oleic acid with DMEM/100 μM oleic acid as a blank for an additional 6 h. Subsequently, the cells were subjected to Oil Red O staining or TC and TG determination as described previously.[42] Each experiment (n = 8 for Oil Red O staining or n = 3 for TC and TG determination) was repeated in triplicate.

2.8. oxLDL-induced foam cell formation.

RAW264.7 cells were maintained in DMEM medium supplemented with penicillin/streptomycin (100 μg/mL) and 10% fetal bovine serum. The cells with 70-80% confluence were incubated with DMEM + oxLDL (50 mg/mL) and individual compound (each, 10 μM) or the positive control rosiglitazone (10 μM) for 12 h. Subsequently, the cells were subjected to Oil Red O staining, photography and TC determination.

2.9. Cholesterol uptake assay.

Cholesterol uptake assays were performed using 25-NBD cholesterol in RAW264.7 macrophages. The cells were plated in 96-well clear-bottom black plates at 4×10^4 cells/well. Six hours later, the medium was removed, and the cells were labeled with 25-NBD cholesterol (5 μg/mL) in aliquots of serum-free DMEM individually containing 10 μM of each of the experimental compounds or an equal volume of DMSO for indicated time. Then, the cells were washed twice with phosphate buffered saline (PBS), and the amounts of cholesterol in the cells were measured using a Tecan Infinite M1000Pro Microplate Reader (TECAN Group Ltd., Shanghai, China; excitation 485 nm, emission 535 nm). Each uptake assay was performed in duplicate in three experiments.

2.10. Cholesterol efflux assay.

RAW264.7 cells were equilibrated with NBD-cholesterol (1 μg/mL) for 12 h. The NBD-cholesterol labeled cells were washed with PBS and incubated in serum-free DMEM medium containing 50 μg/mL HDL and 10 μM of each experimental compounds individually for 6 h. Fluorescence-labeled cholesterol released from the cells into the medium was measured with a Tecan Infinite M1000Pro Microplate Reader (TECAN Group Ltd., Shanghai, China). Cholesterol efflux was expressed as a

219 percentage of fluorescence in the medium relative to the total amounts of fluorescence
220 detected in the cells and the medium. Each experiment was performed in triplicate
221 with 3 replicates each time.

222 **2.11. Quantitative real-time PCR**.

223 Total RNA extraction, cDNA synthesis, and quantitative PCR assays were
224 performed as described previously.[43] Samples were cycled 40 times using a Fast
225 ABI-7500 sequence detector (Applied Biosystems). ABI-7500 cycle conditions were
226 conducted by 5 min at 95 °C, and were followed by 40 cycles of 15 s at 95 °C, 30 s at
227 60 °C, and 30 s at 72 °C. Cycle threshold (CT) was calculated under default settings
228 for real-time sequence detection software (Applied Biosystems). At least three
229 independent biological replicates were performed to check the reproducibility of the
230 data. The gene-specific primers used for quantitative PCR are listed in Table 2.

231 Table 2. Primers used in real-time quantitative PCR analysis.

	Name	Forward (5′-3′)	Reverse (5′-3′)
For HepG2	FAS	CGGTACGCGACGGCTGCCTG	GCTGCTCCACGAACTCAAACACCG
	ACC	TGATGTCAATCTCCCCGCAGC	TTGCTTCTTCTCTGTTTTCTCCCC
	HMGR	GGACCCCTTTGCTTAGATGAAA	CCACCAAGACCTATTGCTCTG
	CPT-1	CGTCTTTTGGGATCCACGATT	TGTGCTGGATGGTGTCTGTCTC
	β-actin	CCTGGCACCCAGCACAAT	GCCGATCCACACACGGAGTACT
For RAW264.7	PPARγ	GCAGCTACTGCATGTGATCAAGA	GTCAGCGGGTGGGACTTTC
	LXRα	AGGAGTGTCGACTTCGCAAA	CTCTTCTTGCCGCTTCAGTTT
	ABCG1	CAAGACCCTTTTGAAAGGGATCTC	GCCAGAATATTCATGAGTGTGGAC
	CD36	CAAGCTCCTTGGCATGGTAGA	TGGATTTGCAAGCACAATATGAA
	SR-1	TTAAAGGTGATCGGGGACAAA	CAACCAGTCGAACTGTCTTAAG
	β-actin	ACACTGTGCCCATCTACGAG	CAGCACTGTGTTGGCATAGAG

232 **2.12. Western blot**

233 HepG2 cells were lysed in lysis buffer containing 10% glycerol, 1% Triton X-100,
234 135 mM NaCl, 20 mM Tris (pH 8.0), 2.7 mM KCl, 1 mM $MgCl_2$, and protease and
235 phosphatase inhibitors (0.5 mM PMSF, 2 μM pepstatin, and 2 μM okadaic acid).
236 Aliquots of samples were subjected to SDS-PAGE followed by transfer to
237 polyvinylidenedifluoride (PVDF) membranes. Immunoblotting was performed using

respective antibodies (1:1000). Following incubation with horseradish peroxidase-conjugated secondary antibody, proteins were detected with ECL plus kits.

2.13. Measurement of PPARγ promoter activity

A transactivation reporter assay in 293T cells was performed. Briefly, cells were transiently transfected with a PPARγ expression vector and a DR-1 luciferase reporter vector. At 6 h after transfection, the transfection mixture was replaced with fresh medium containing the appropriate agonist. Luciferase assays were performed after 24 h using a luciferase assay kit according to the manufacturer's instructions.

2.14. Cell viability assay

Cell viability was examined using an MTT assay. RAW264.7 macrophages in 96-well culture plates were treated with compounds with 50 μM digitonin as a cytotoxic control. The cells were incubated for 12 h, and MTT reagent (5 mg/mL) was added to each well. After2 h, the medium was removed and cells were lysed in 200 μL of DMSO. The absorbance at 565 nm was measured using a microplate reader (TECAN Group Ltd., Shanghai, China).

2.15. Statistical analyses

The data are presented as the mean ± SEM. Differences were assessed by one-way analysis of variance (ANOVA) followed by Dunnett's*post hoc* test. A probability level (p) of 0.05 was considered significant. SPSS 17.0 for Windows (SPSS, Chicago, IL, USA) was used for statistical analysis.

3. Results and discussion

3.1. Structural elucidation

Compound **1** had a molecular formula of $C_{21}H_{24}O_7$, as determined by the HRESIMS (m/z 389.1594 $[M + H]^+$, calcd. 389.1600) and NMR data, requiring ten degrees of unsaturation. ^{1}H NMR spectrum exhibited the resonances for three methyl groups,

four aromatic protons belonging to *meta*- and *ortho*-spin systems, and a number of alkyl protons. The ^{13}C NMR spectrum provided a total of 21 carbon resonances (Table 1), including 12 aromatic carbons for two phenyl rings and a carbonyl carbon. Analyses of 2D NMR (COSY, HMQC and HMBC) data established the basic skeleton of **1** to be a diphenyl ether lactone, closely related to the structure of penicillide.[27] The distinction was only attributed to the substitution at isopentyl side chain, in which a hydroxyl group at C-5′ (δ_C 69.4) was assigned by the HMBC correlations from H_3-4′ (δ_H 0.90, d) to C-3′ (δ_C 33.8) , C-2′ (δ_C 43.2) and C-5′, in addition to the COSY correlation from H-3′ (δ_H 1.78, m) to H_2-5′ (δ_H 4.36), H_3-4′ and H_2-2′. The configuration of C-1′ was determined on the basis of the revised Mosher method.[28] Firstly, the phenolic group at C-11 was protected by the methylation with dimethyl carbonate (DMC),[29] and then the esterification of the 11-methylated **1** with (*R*)-MPA and (*S*)-MPA was accomplished. Calculation of the $\Delta\delta$ ($\delta_R-\delta_S$) data of (R)- and (S)-MPA esters of the 11-methylated **1** (Fig. 2) conducted the configuration of C-1′ to be *S*. In addition, the absolute configuration at C-3′ was established according to the methodology reported by Riguera and co-workers for determining the absolute configuration of *β*-chiral primary alcohols.[30] 11-Methylated **1** was reacted with (*R*)- and (*S*)-2-(anthracen -9-yl)-2-methoxyacetic acid (9-AMA) to form 9-AMA esters. Calculation of $\Delta\delta$ ($\delta_R-\delta_S$) values obtained from the *R*- and *S*-ester derivatives **1c** and **1d** led to an *S*-configuration assigned at C-3′. Thus, the structure of **1** was assigned to 5′-hydroxypenicillide.

Inspection of spectroscopic data and the comparison of the NMR data and specific rotation resulted in the structures of 15 known phenolic metabolites to be identical to penicillide (**2**),[27] isopenicillide (**3**),[31] dehydroisopenicillide (**4**),[27]

1-dehydroxypencillide (**5**),[27] vermixocin B (**6**),[32] methyl tenellate (**7**),[33] secopenicillide A (**8**),[34] talaromycin C (**9**),[35] deacetyl talaromycin C (**10**),[35] deoxyfunicone(**11**),[36] funicone (**12**),[37] 3-O-methylfunicone (**13**),[38] vermistatin (**14**),[39] hydroxyvermistatin (**15**),[40] and methoxyvermistatin (**16**).[41] Based on their scaffolds, these compounds are classified to penicillide-type，tenellic acid-type, funicone-type, and vermistatin-type.

During the separation process, a spirolactone purpactin C[41] was isolated as an unstable component, which was able to convert to secopenicillide A (**8**). The penicillide-type analogues such as vermixocin B (**6**) was likely derived from **8** via the reduction of aldehydic group to form an alcohol intermediate, and then the esterification was occurred. In addition, the structural relationship of remaining diphenyl ethers was depicted by the occurrence of deacetylation, hydroxylation, methylation, and dehydration (Fig. 3).

3.2. Pharmacological activity

3.2.1. Lipid-lowering effect

Compounds **1-16** were tested for the inhibitory effects against oleic acid (OA)-elicited lipid accumulation in HepG2 liver cells. Prior to the test, the cytotoxic activity of all compounds toward HepG2 cells was evaluated by the MTT assay, while all compounds showed weak or no cytotoxic effects with the $IC_{50} > 50$ μM. The lipid-lowering test revealed that eight compounds (**4**, **7-8**, **11-15**) exerted the inhibitory effects against lipid accumulation at a dose of 10 μM as measured by Oil Red O staining (Fig. 4). Analyses of primary structure-activity relationship conducted to recognize the weak activity of penicillide-type analogues with the exception of **4**, which was characterized by the presence of a hydroxyisoprenyl group. In regard to

tenellic acid-type analogues, the substitution of side chain and functional group at ring A directly affected the inhibitory effect. The analogues with a dimethoxymethane (**9**) to replace an aldehydic group (**9** vs.**10**, OD: 0.278 vs. 0.276) or with an acetoxy group instead of hydroxyl group at side chain (**10** vs. **8**, OD: 0.276 vs. 0.267) reduced activity. Funicone-type analogues are more effective among the tested compounds, while **11** (OD: 0.264) exhibited the effect more potent than its analogues **12** (OD: 0.272) and **13** (OD: 0.271) which were modified with hydroxyl or methoxy group at C-3. vermistatin-type analogues **14-16** with a γ-lactone unit showed more effective than that of **11**, indicating the γ-lactone unit being a functional group for lipid-lowering function.

3.2.2. Compounds decrease TC and TG levels and regulate lipogenic genes

Further investigation revealed that five compounds (**4**, **11**, **13-15**) significantly suppressed intracellular total cholesterol (TC) levels (Fig. 5A) and intracellular triglycerides (TG) (Fig. 5B), of which **4**, **13-15** were more potent than the positive control simvastatin, a marketed anti-hyperlipidemic drug. In order to uncover whether lipid-lowering effects of the active compounds related to key lipogenic genes, a real-time quantitative PCR experiment was performed. The experimental data conducted compounds **4**, **11**, **13-15** dramatically down-regulating fatty acid synthase (FAS), acetyl-CoA carboxylase (ACC) and 3-hydroxy-3-methylglutaryl-CoA reductase (HMGR) at the mRNA levels (Fig. 6), whereas these compounds significantly up-regulated the lipid catabolic gene carnitinepalmitoyl transterase-1 (CPT-1). These findings indicated that the lipid-lowering effects of compounds (**4**, **11**, **13-15**) to be induced by the inhibition of lipogenesis and the stimulation of lipid catabolism.

3.2.3. Compounds decrease oxLDL-induced lipid overaccumulation in

RAW264.7 cells

Foam cell formation conducted the elevation of macrophage cholesterol levels and imbalanced lipid efflux and influx, leading atherosclerotic lesions. Therefore, detection of the lipid-lowering active compounds against foam cell formation in RAW264.7 macrophages as induced by oxLDL directly reflected the inhibitory effects against atherosclerosis. We established a model of foam cell formation accounting for macrophage RCT. This model is presented as a system of non-linear ordinary differential equations to be motivated by observations of time scales for oxidation of lipids and MRCT. The bioassay results revealed that compounds **4**, **8**, **11**, and **13-16** significantly reduced oxLDL-stimulated lipid accumulation in RAW264.7 cells in a dose of 10 μM, reflecting their effects to prevent oxLDL-induced foam cell formation in RAW264.7 macrophages. In addition, compounds **4** and **15** exhibited potent effects which were comparable to that induced by the positive control rosiglitazone at the same dose (10 μM) (Figures 7A). Cell surface enlargement is an additional sign to detect the formation of foam cell. Therefore, an evaluation assay consisting of photography after Oil Red O-staining was performed. Compounds **4**, **8**, **11**, and **13-16** largely alleviated neutral lipid accumulation, and reduced the cell surface area (Fig. 7B).

Lipid dysregulation is a key factor to induce atherosclerosis, a major risk of cardiovascular disease (peripheral arterial disease, coronary heart disease, stroke, and heart attack). Macrophage derived foam cells are a major constituent of the fatty deposits characterizing the disease atherosclerosis. Foam cells are formed when certain immune cells (macrophages) take on oxidized low density lipoproteins (oxLDL) through failed phagocytosis. High density lipoproteins (HDL) are known to

have a number of anti-atherogenic effects. One of these stems from their ability to remove excess cellular cholesterol for processing in the liver-a process called reverse cholesterol transport (RCT). HDL induced macrophage RCT by forming foam cells and removing excess lipids by efflux transporters.

3.2.4. Compounds inhibit cholesterol uptake in RAW264.7 macrophages

Among these active compounds, compounds **4**, **11**, **14-16** dramatically decreased the intracellular total cholesterol levels, whereas **8** and **13** were inactive (Fig. 8A). These results suggested that compounds **4**, **11**, **14-16** were adequate in cholesterol uptake or cholesterol efflux to high density lipoprotein (HDL). Real-time quantitative PCR were performed to determine the mechanism of compounds to regulate the cholesterol dynamics and the expressions of cholesterol efflux/influx-modulating genes. Similar to 25-NBD cholesterol, compounds **11**, **14-16** dramatically inhibited cholesterol uptake in RAW264.7 macrophages in a dose-dependent manner (Fig. 8B), while compounds **4**, **14-16** significantly stimulated cholesterol efflux to HDL (Fig. 8C). The efficiencies of **4** and **15** for cholesterol efflux (FI: 63.92% and 64.88%) showed more potent than that of rosiglitazone (FI: 63.38%). In addition, compounds **14** and **16** showed significant activity to inhibit cholesterol influx (FI: 62.39% and 60.26%), but they exerted weaker effect than rosiglitazone (FI: 63.38%±0.30%) (Fig. 8B and 8C).

3.2.5. Compounds regulate mRNA levels of cholesterol efflux/influx-modulating genes and PPARγ transcriptional activity

The critical scavenger receptors CD36 and SR-1 are the main targets to regulate cholesterol dynamics such as cholesterol uptake, while peroxisome proliferator-activatedreceptor-γ (PPARγ), liver X receptor-α (LXRα) and

ATP-binding cassette G1 (ABCG1) play key role to stimulate cholesterol efflux. Compounds **14-16** (10 μM) significantly induced down-regulation of CD36 and SR-1 transcription, while compound **11** only decreased the mRNA level of CD36. However, compound **4** was inactive toward the two cholesterol influx stimulators (Fig. 9). These findings suggested that the compounds with different scaffolds undertook distinct mechanism for the cholesterol uptake. Moreover, compounds **4** and **15** dramatically increased the mRNA levels of PPARγ, LXRα and ABCG1 (Fig. 9), indicating the promoting cholesterol efflux of the two compounds closely related to the cholesterol efflux stimulators. Compounds **14** and **16** were effective in promoting cholesterol efflux but showed no significant effects on the transcription of these three cholesterol efflux stimulators, suggesting that the two compounds may stimulate cholesterol efflux via currently unknown mechanism.

4. Conclusions

In summary, this is the first report of diphenyl ethers and related natural products, which were potent for lipid-lowering effects and inhibition of foam cell formation. These findings suggested them to be the potential leads against hyperlipidemia and atherosclerosis. Mechanistic study revealed the inhibition of intracellular total cholesterol (TC) levels and intracellular triglycerides (TG) of compounds **4**, **11**, **13-15** related to down-regulation of fatty acid synthase (FAS), acetyl-CoA carboxylase (ACC) and 3-hydroxy-3-methylglutaryl-CoA reductase (HMGR) and the up-regulation of the lipid catabolic gene carnitinepalmitoyl transterase-1 (CPT-1). The suppression of oxLDL-induced foam cell formation by compounds **4**, **11**, **14-16** *via* inhibiting cholesterol influx was induced by the down-regulation of CD36 and SR-1 or promoting cholesterol efflux by upregulation of PPARγ, LXRα and ABCG1.

Present work provided a group of new chemical entity to be promising for the development of antihyperlipidemic and antiatherosclerosis agents.

Acknowledgments

This work was supported by the National Basic Research Program 973(2015CB755906), the NSFC-Shangdong Joint Fund for Marine Science (U1406402), the National Hi-Tech863-Projects (2011AA090701, 2013AA092902), COMRA (DY125-15-T-01), and National Natural Science Foundation of China (41376127, 81573436).

Notes and References

1. K. M. Patel, A. Strong, J. Tohyama, X. Jin, C. R. Morales, J. Billheimer, J. Millar, H. Kruth and D.J. Rader, *Circ. Res.*, 2015, **116**, 789-796.
2. J. S. Kishor, M. K. Kathivarin and S. Rahul, *Bioorg. Med. Chem.*, 2007, **15**, 4674-4699.
3. S. M. Grundy, G. J. Balady and M. H. Criqui, *Circulation*,1998, **97**, 1876-1887.
4. W. F. Keane, J. Peter and B. L. Kasiske, *Kidney Int. Suppl.*, 1992, **38**, S134-141.
5. M. J. Veerkamp, J. Graaf, S. J. H. Bredie, J. C. M Hendriks, P. N. M. Demacker and A. F. H Stalenhoef, *Arterioscler Thromb Vasc Biol.*, 2002, **22**, 274-282.
6. R. L. Satarasinghe, R. Ramesh, A. A. A. Riyaaz, P. A. K. G. Gunarathne and A. P. Silva, *Drug Metabol. Drug Interact.*, 2007, **22**, 279-283.
7. L. Fernandez-Friera, J. L. Penalvo, A. Fernandez-Ortiz, B. Ibanez, B. Lopez-Melgar, M. Laclaustra, B. Oliva, A. Mocoroa, J. Mendiguren, V.M. de Vega, L. García, J. Molina, J. Sánchez-González, G. Guzmán, J. C. Alonso-Farto, E. Guallar, F. Civeira, H. Sillesen, S. Pocock, J.M. Ordovás, G. Sanz, L. J. Jiménez-Borreguero and V. Fuster, *Circulation*, 2015, **131**, 2104-2113.
8. R. Ladeiras-Lopes, S. Agewall, A. Tawakol, B. Staels, E. Stein, R.J. Mentz, A. Leite-Moreira, F. Zannad and W. Koenig, *Int. J. Cardiol.*, 2015, **192**, 72-81.
9. S. Mendis and O. Chestnov, *Curr. Cardiol. Rep.*, 2014, **16**, 486.
10. K. M. Patel, A. Strong, J. Tohyama, X. Jin, C. R. Morales, J. Billheimer, J. Millar, H. Kruth and D.J. Rader, *Circ. Res.*, 2015, **116**, 789-796.
11. L. N. Rao, T. Ponnusamy, S. Philip, R. Mukhopadhyay, V.V. Kakkar and L. Mundkur, *Lipids*, 2015, **50**, 785-797.
12. X. H. Yu, Y. C. Fu, D. W. Zhang, K. Yin and C.K. Tang, *Clin. Chim. Acta*, 2013, **424**, 245–252.

13. S. O. Rahaman, W. Swat, M. Febbraio and R.L. Silverstein, *J. Biol. Chem.*, 2011, **286**, 7010–7017.

14. G. J. Zhao, K. Yin, Y.C. Fu and C.K. Tang, *Mol. Med.*, 2012, **18**, 149–158.

15. J. Y. Lee, J. Karwatsky, L. Ma and X. Zha, *Am. J. Physiol. Cell Physiol.*, 2011, **301**, C886–894.

16. M.A. Kennedy, G.C. Barrera, K. Nakamura, A. Baldan, P. Tarr, M.C. Fishbein, J. Frank, O.L. Francone and P.A. Edwards, *Cell Metab.*, 2005, **1**, 121–131.

17. A. Ji, J.M. Wroblewski, L. Cai, M.C. de Beer, N.R. Webb and D.R. van der Westhuyzen, *J. Lipid Res.*, 2012, **53**, 446–455.

18. L. Yvan-Charvet, N. Wang and A.R. Tall, *Arterioscler. Thromb. Vasc. Biol.*, 2010, **30**, 139–143.

19. A. Chawla, W.A. Boisvert, C.H. Lee, B.A. Laffitte, Y. Barak, S.B. Joseph, D. Liao, L. Nagy, P.A. Edwards, L.K. Curtiss, R.M. Evans and P. Tontonoz, *Mol. Cell*, 2001, **7**, 161–171.

20. G. Chinetti, S. Lestavel, V. Bocher, A.T. Remaley, B. Neve, I.P. Torra, E. Teissier, A. Minnich, M. Jaye, N. Duverger, H.B. Brewer, J.C. Fruchart, V. Clavey and B. Staels, *Nat. Med.*, 2001, **7**, 53–58.

21. A. Ravelli, *Arthritis Rheum.*, 2012, **64**, 33–36.

22. K. Pahan, *Cell Mol. Life Sci.*, 2006, **63**, 1165–1178.

23. A. Endo, M. Kuroda, and Y. Tsujita, *J. Antibiot*., 1976, **29**, 1346–1348.

24. A. Endo, *J. Med. Chem.*, 1985, **28**, 401-405.

25. C. J. Vaughan and A. M. Jr. Gotto, n statins: 2003. *Circulation*, 2004, **110**, 886–892.

26. E.S. Stroes, P.D. Thompson, A. Corsini, G.D. Vladutiu, F.J. Raal, K.K. Ray, M. Roden, E. Stein, L. Tokgozoglu, B.G. Nordestgaard, E. Bruckert, G. De Backer,

R.M. Krauss, U. Laufs, R.D. Santos, R.A. Hegele, G.K. Hovingh, L.A. Leiter, F. Mach, W. März, C.B. Newman, O. Wiklund, T.A. Jacobson, A.L. Catapano, M.J. Chapman and H.N. Ginsberg, *Eur. Heart J.* 2015, **36**, 1012–1022.

27. K. Suzuki, K. Nozawa, S. Udagawa, S. Nakajima and K. Kawai, *Phytochemistry* 1991, **30**, 2096-2098.

28. T. Amagata, A. Amagata, K. Tenney, F.A. Valeriote, E. Lobkovsky, J. Clardy and P. Crews, *Org. Lett.* 2003, **5**, 4393–4396.

29. R. Bernini, F. Crisante and M. C. Ginnasi, *Molecules* 2011, **16**, 1418-1425.

30. F. Freire, J. M. Seco, E. Quiñoá, R. Riguera, *Chem. Commun.*, 2007, 1456−1458.

31. D. Zhao, C. Shao, Q. Zhang, K. Wang, F. Guan, T. Shi and C. Wang, *J. Nat. Prod.*, 2015, **78**, 2310-2314.

32. B. Prokas, D. Uhrin, J. Adamcova and J. Fuska, *J. Antibiot.* 1992, **45**, 1268-1272.

33. H. Oh, T.O. Kwon, J.B. Gloer, L. Marvanova and C.A. Shearer, *J. Nat. Prod.*, 1999, **62**, 580-583.

34. S. Komai, T. Hosoe, T. Itabashi, K. Nozawa, T. Yaguchi, K. Fukushima and K. Kawai, *J. Nat. Med.*, 2006, **60**, 185-190.

35. M. Chen, L. Han, C. Shao, Z. She and C. Wang, *Chem Biodivers*., 2015, **12**, 443-450.

36. T. Sassa, M. Nukina and Y. Suzuki, *Agr. Biol. Chem.* 1991, **55**, 2415-2416.

37. L. Merlini, G. Nasini and A. Selva, *Tetrahedron*, 1970, **26**, 2739-2749.

38. S. De Stefano, R. Nicoletti, A. Milone and S. Zambardino, *Phytochemistry*, 1999, **52**, 1399-1401.

39. N. Murtaza, S.A. Husain, T.B. Sarfaraz, N. Sultana and S. Faizi, *Planta Medica*, 1997, **63**, 191.

40. Y. Liu, G. Xia, H. Li, L. Ma, B. Ding, Z. She, Y. Lu, L. He and X. Xia, *Planta*

Medica, 2014, **80**, 912-917.

41. Z. Liu, G. Xia, S. Chen, Y. Liu, H. Li and Z. She, *Mar drugs*, 2014, **12**, 3669-3680.

42. C. Wu, Y. Guo, Y. Su, X. Zhang, H. Luan, X. Zhang, H. Zhu, H. He, X. Wang, G. Sun, X. Sun, P. Guo and P. Zhu, *Cell Mol. Med.*, 2014, **18**, 293-304.

43. C. Wu, X. Zhang, X. Zhang, H. Luan, G. Sun, X. Sun, X. Wang, P. Guo and X. Xu, *J. Nutr. Biochem.* 2014, **25**, 412-419.

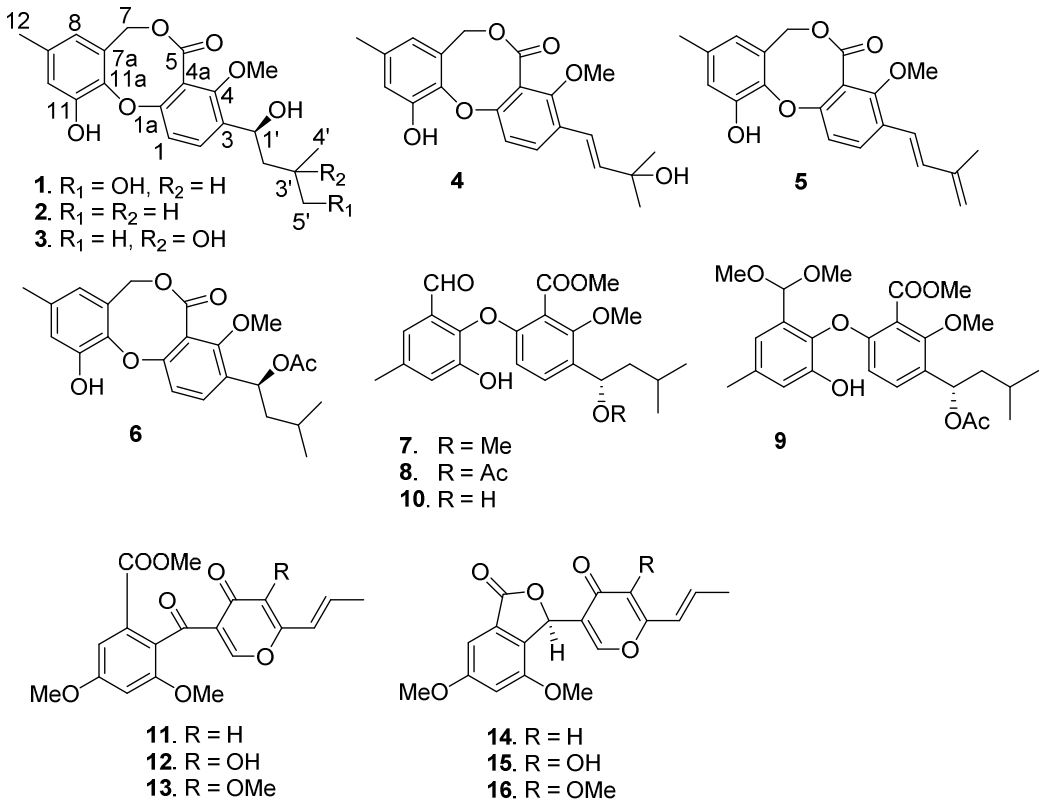

Figure 1 Structures of the isolated compounds

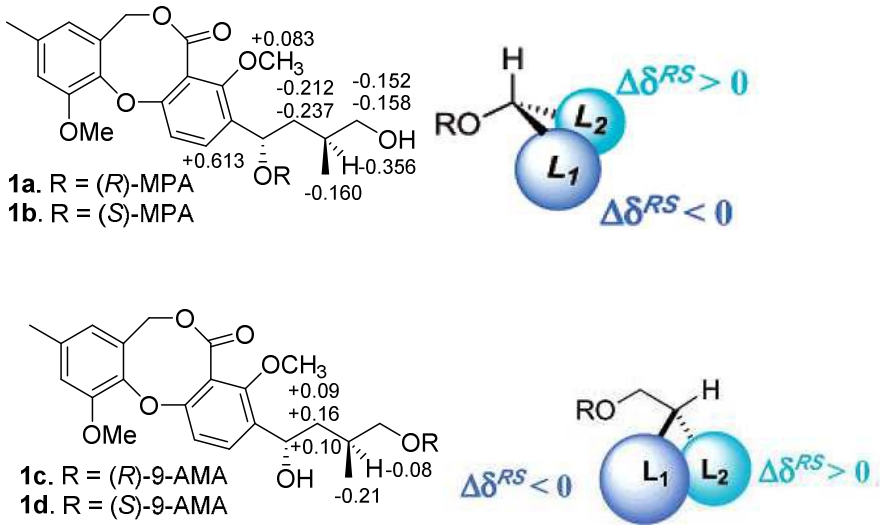

Figure 2. $\Delta\delta$ ($\delta_R-\delta_S$) values (in ppm) for the MPA esters and 9-AMA esters of **1**

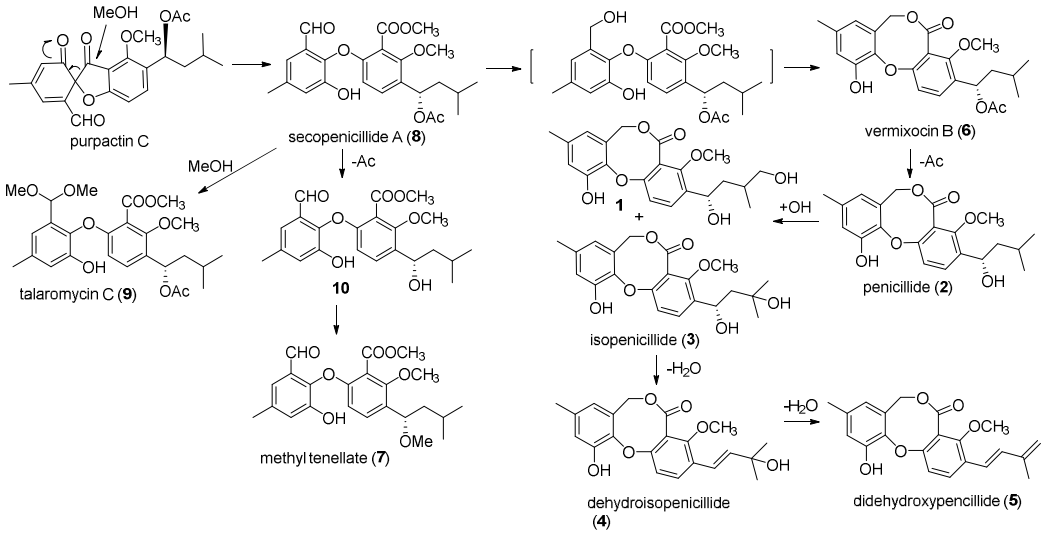

Figure 3. Postulation of the biogenetic relationship of the isolated compounds

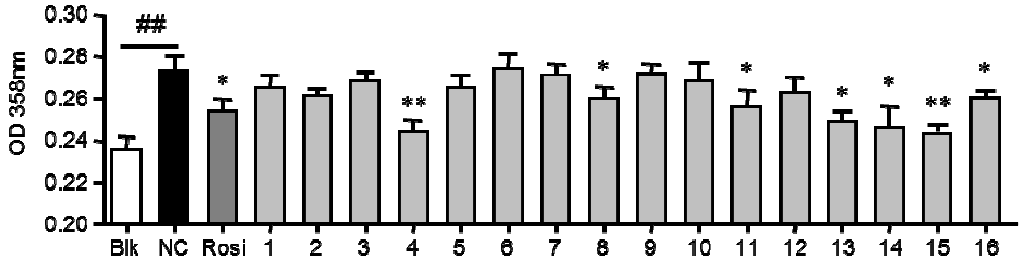

Figure 4. Spectrophotometry at 358 nm after Oil Red O staining.
The dose of compounds and simvastatin (Simv) were 10 μM. The blank group (Blk) was given DMEM only while other groups were given 100 μM of OA to elicit lipid accumulation. Bars depict the means ± SEM in triplicate. $^{\#\#}p< 0.01$, $^{\#\#\#}p< 0.001$ blank group vs negative control; $^{*}p< 0.05$, $^{**}p< 0.01$, $^{***}p< 0.001$, test group vs negative control group. Blk: blank group; NC: negative control; Simv: simastatin.

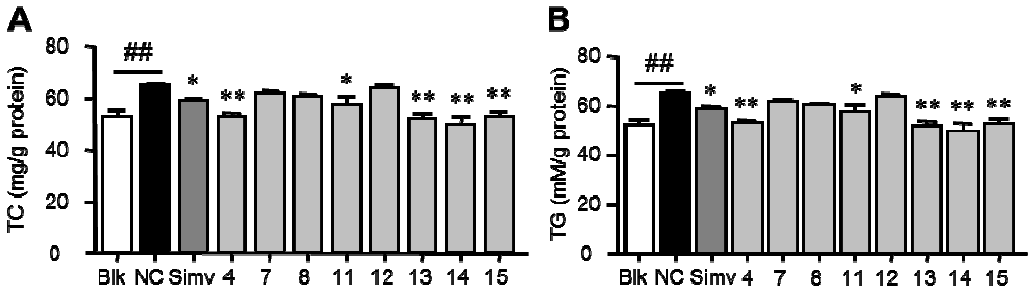

Figure 5. Compounds inhibit lipid accumulation in oleic acid (OA)-elicited HepG2 cells. (A) and (B) intracellular levels of total cholesterol (TC) and triglycerides (TG)

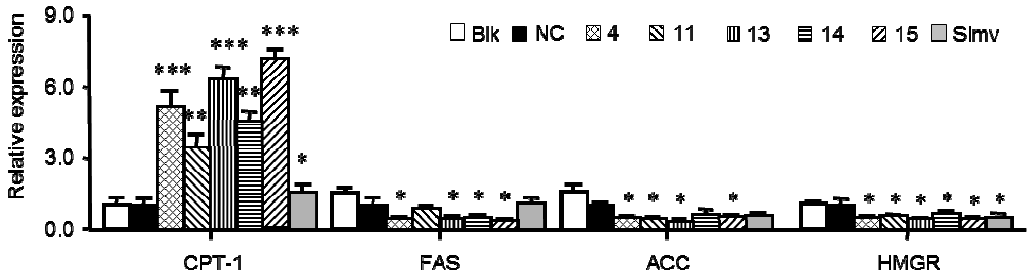

Figure 6. mRNA levels of key lipid metabolic genes determined by real-time quantitative PCR with β-actin as internal control.

The concentrations of the compounds and simvastatin (Simv) were 10 μM. The blank group (Blk) was given DMEM only while other groups were given 100 μM of OA to elicit lipid accumulation. Bars depict the means ± SEM in triplicate. $^{\#\#}p< 0.01$, $^{\#\#\#}p< 0.001$ blank group vs negative control; $^{*}p< 0.05$, $^{**}p< 0.01$, $^{***}p< 0.001$, test group vs negative control group. Blk: blank group; NC: negative control; Simv: simastatin.

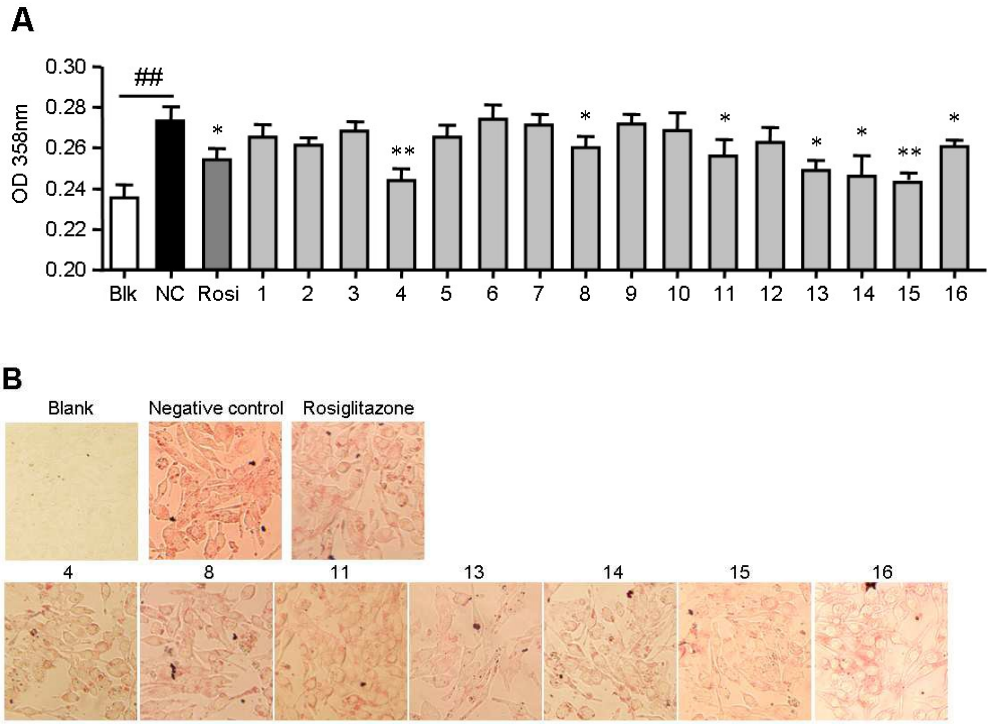

Figure 7. Compounds suppress oxLDL-induced foam cell formation in RAW264.7 macrophages.

(A) Spectrophotometry at 358 nm after Oil Red O staining; (B) phenotype of foam cell induced by compounds. The concentrations of the compounds and rosiglitazone (Rosi) were 10 μM. The blank group was given DMEM only while other groups were given 50 μg/ml of oxLDL to induce foam cell formation. Bars depict the means ± SEM in triplicate. $^{\#\#}p < 0.01$ blank group vs negative control; $^{*}p < 0.05$, $^{**}p < 0.01$, $^{***}p < 0.001$, test group vs negative control group. Blk: blank group; NC: negative control; Rosi: rosiglitazone.

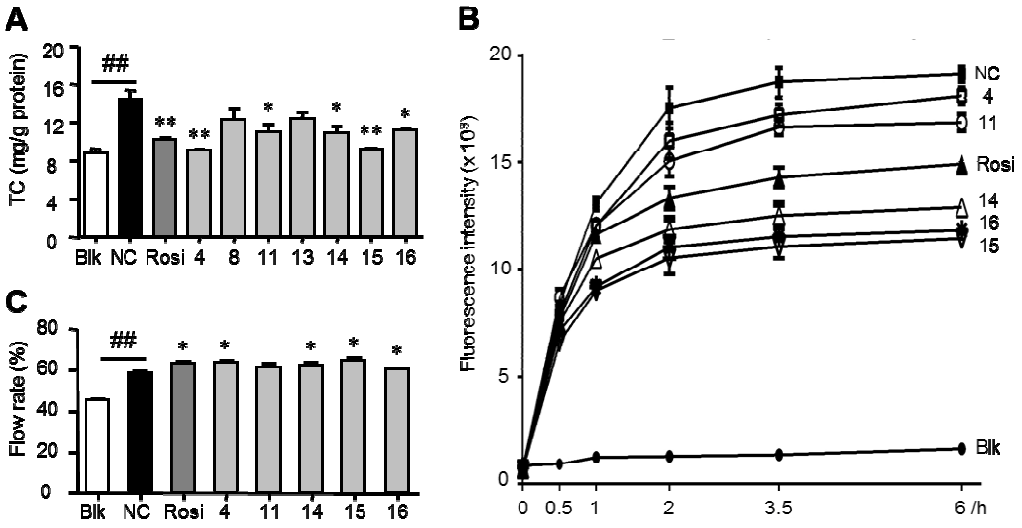

Figure 8. Compounds suppress intracellular total cholesterol (TC) accumulation and regulate cholesterol influx/efflux in RAW264.7 macrophages.

(A) Intracellular TC levels; (B) time-dependent cholesterol uptake curves indicated by NBD-cholesterol; (C) NBD-cholesterol efflux to HDL;

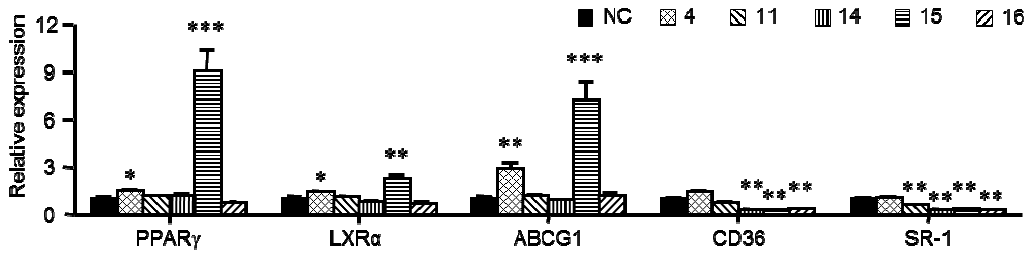

Figure 9. Effects of compounds **4**, **11**, **14-16** on the mRNA levels of PPARγ, LXRα, ABCG1, CD36 and scavenger receptor-1 (SR-1) in RAW264.7 cells.

Real-time PCR was conducted with gene-specific oligonucleotide primers. The amplification of β-actin served as an internal control. The values shown are the means ± SEM of at least three experiments. * $p < 0.05$, ** $p < 0.01$, *** $p < 0.001$ *vs.* control.

Table **1** ^{1}H and ^{13}C NMR data of **1**

No.	1	
	δ_H (ppm, *J* in Hz)	δ_C (ppm)
1	6.96, d (8.4)	118.0 CH
2	7.65, d (8.4)	131.6 CH
3		134.4 C
4		153.7 C
4a		119.5 C
5		167.8 C
7	5.08, s	69.1 CH_2
7a		127.5 C
8	6.34, d (1.6)	120.3 CH
9		138.7 C
10	6.77, d (1.6)	118.7 CH
11		148.9 C
11a		142.2 C
1a		151.4 C
13	2.16, s	20.8 C
1'	4.93, dd (3.0, 8.6)	64.3 CH
2'	1.21, m; 1.60, m	43.2 CH_2
3'	1.78, m	33.8 CH
4'	0.90, d (6.7)	22.1 CH_3
5'	4.36, d (6.0)	69.4 CH_2
OMe	3.80, s	62.4 CH_3
11-OH	9.68, s	

[a]Measured in DMSO-d_6 at 400 MH for ^{1}H and 100MHz for ^{13}C

TOC